A PRIMER ON THE AGEOSTROPHIC WIND

Scott M. Rochette

Department of the Earth Sciences
State University of New York, College at Brockport
Brockport, New York

Patrick S. Market

Department of Soil, Environmental and Atmospheric Sciences
University of Missouri-Columbia
Columbia, Missouri

Abstract

The ageostrophic wind is an essential component of the synoptic-scale and mesoscale atmospheric environments, yet is often overlooked. A review of the underlying theory is presented, along with a derivation of the expression for the ageostrophic wind. This expression is partitioned into three separate components, along with discussions of their physical significance. A case study is offered to further illustrate these concepts.

1. Introduction

The ageostrophic wind is paramount in operational meteorology, but not likely given much thought. It can be argued that if the atmosphere were purely geostrophic, there would be no need to forecast the weather (and, therefore, no need for weather forecasters), as it would never change.

The existence of the (albeit small) ageostrophic wind is the underlying premise for quasi-geostrophic (Q-G) theory, discussed especially well in a series of articles by Billingsley (1996, 1997, 1998), which were published in this journal. If not for the ageostrophic wind, convergence and divergence fields would be significantly weaker (the geostrophic wind is often assumed to be nondivergent), and mid-latitude weather systems would not grow, develop, and decay in the fashion to which we have become accustomed.

The purpose of this article is to illustrate the theory and application of the ageostrophic wind. Although it is generally small for synoptic-scale motions (i.e. the "real" synoptic-scale atmosphere is never far from geostrophic balance), the fact that it is non-zero has dramatic implications for operational meteorology, most notably the creation of divergent and convergent regions. These areas are responsible for the growth, development, and decay of weather systems, especially in the mid-latitude and polar regions. Section 2 outlines the theory of the geostrophic wind and its implications, while Section 3 provides the derivation of the ageostrophic wind expression. Section 4 is a development and examination of the individual right-hand side (RHS) terms of the ageostrophic wind expression. A recent case study serves as a bridge between theory and application in Section 5, with a concluding discussion provided in Section 6. A brief review of vector functions and a proof of the "non-divergent" nature of the geostrophic wind are provided as Appendices 1 and 2, respectively.

2. Basic Theory

a. Definition of the ageostrophic wind

The simplest definition of the ageostrophic wind, i.e. the portion of the real (observed) vector wind that departs from geostrophy, is shown in the following expression:

$$\vec{V} = \vec{V}_g + \vec{V}_{ag} \Rightarrow \vec{V}_{ag} = \vec{V} - \vec{V}_g \tag{1}$$

where $\vec{V}$ represents the real (observed) vector wind, $\vec{V}_g$ represents the geostrophic wind vector, and $\vec{V}_{ag}$ is the ageostrophic wind vector. This expression states that the observed wind is the vector sum of the geostrophic and ageostrophic wind vectors (see Fig. 1).

b. The geostrophic wind

In order to examine the ageostrophic wind and its role in meteorology in greater detail, the geostrophic wind must first be defined:

$$\begin{aligned} \frac{1}{\rho}\frac{\partial p}{\partial x} &= fv_g \\ \frac{1}{\rho}\frac{\partial p}{\partial y} &= -fu_g \end{aligned} \tag{2}$$

$$\vec{V}_g = \frac{\hat{k}}{\rho f} \times \nabla p = \frac{\hat{k}}{f} \times \nabla \Phi \tag{3}$$

Expressions (2) and (3) are various representations of the geostrophic wind. Expression (2) represents the horizon-

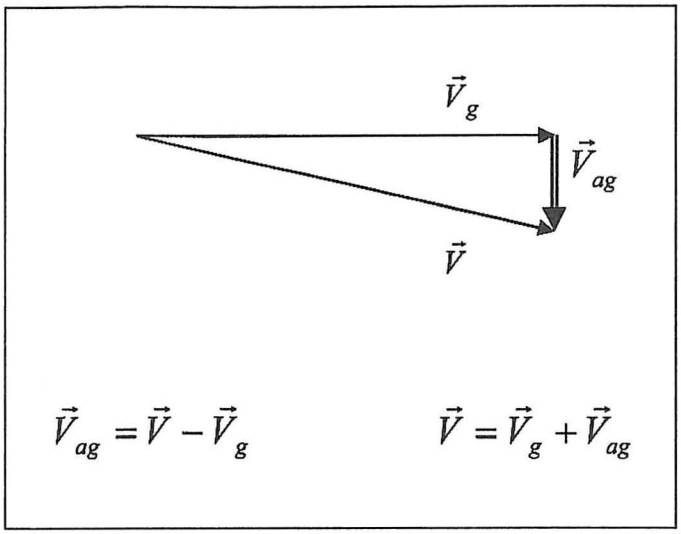

Fig. 1. Relationship between the real wind ($\vec{V}$), the geostrophic wind ($\vec{V}_g$), and the ageostrophic wind ($\vec{V}_{ag}$).

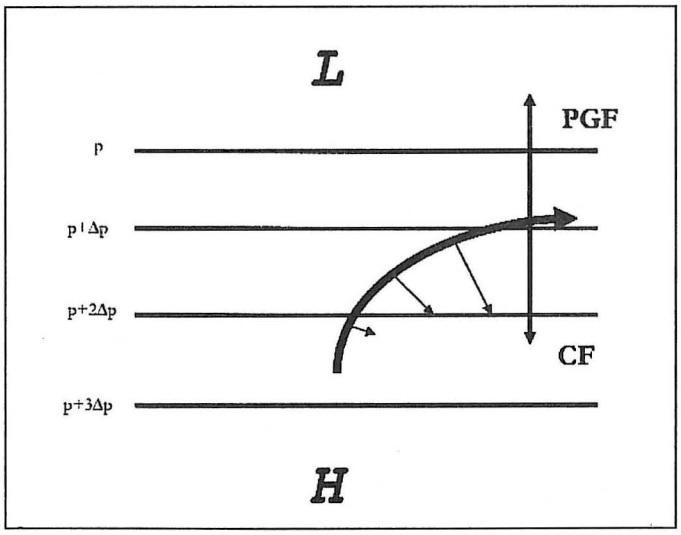

Fig. 2. Approach to geostrophic balance for a parcel initially at rest. Heavy curved arrow represents the parcel's trajectory as it undergoes geostrophic adjustment, small arrows represent Coriolis force. **PGF** is the pressure gradient force, whereas **CF** is the Coriolis force (Hess 1959).

tal geostrophic wind in Cartesian form, decomposed into its east-west (u_g) and g north-south (v_g) components, while (3) is the vector form of the geostrophic wind. The term f represents the Coriolis parameter (see below), ρ is density, p is pressure, Φ represents geopotential (see Appendix 1 for definition), x and y represent the east-west and north-south directions, respectively, and $\hat{k}$ represents the unit vector in the vertical direction.

Notice, especially from (2), that the geostrophic wind is the result of a balance between two forces, pressure gradient force (PGF) and Coriolis force (CF). The geostrophic wind blows parallel to isobars or height contours, with lower pressure/heights to the *left (right)* of the flow in the northern (southern) hemisphere, via the Buys-Ballot law. This is due to the (eventual) balance between the PGF and the CF. The PGF causes air to accelerate from a standstill and move from higher to lower pressure, while the CF acts only to deflect the air to the right (left) of its intended path in the northern (southern) hemisphere (no effect on speed). Note, however, that the CF gets stronger as the wind speed increases (see Fig. 2). The speed of the geostrophic wind is determined solely by the strength of the PGF, which is directly proportional to the magnitude of the pressure gradient (i.e. strong ∇p or $\nabla\Phi$ = faster geostrophic wind).

The geostrophic wind most closely approximates the synoptic-scale observed wind in the mid-latitude and polar regions, where the Coriolis force is strong. Recall the expression for Coriolis parameter f:

$$f = 2\Omega \sin\phi \qquad (4)$$

In this expression, Ω represents the angular rotation rate of the earth (7.292×10^{-5} s^{-1}), which can be considered constant. The term ϕ represents latitude, which is minimized at the equator (0°) and reaches a maximum at either of the poles (90° N or S). As such, the geostrophic approximation works best in middle and high latitudes.

In addition, vertical location (altitude) is important. The geostrophic approximation works best at higher altitudes, away from the *atmospheric boundary layer (ABL)*, the lowest 1 km (give or take) of the atmosphere where friction must be taken into account. Recall that friction is a retarding force, acting in the direction opposite that of the motion.

The geostrophic approximation also requires *straight* isobars or height contours. Once the contours have curvature, then the centripetal acceleration must be taken into account. The three-way balance between the PGF, CF, and the centripetal acceleration results in the gradient wind. (Note that the PGF and CF are considered *specific* forces, i.e. force per unit mass, and as such can be expressed in units of acceleration.)

With all of this in mind, large-scale (synoptic-scale) motions above the ABL in the mid-latitude and polar regions are closely approximated by the geostrophic wind. The observed wind at sufficiently high latitudes and altitudes is usually parallel to the isobars/height contours, and its speed is usually within 15% of the geostrophic wind speed (determined by the magnitude of ∇p). This state is described as *quasi-geostrophic* (Wallace and Hobbs 1977). This means that for such motions, the magnitude of the ageostrophic wind is small, relative to the observed or geostrophic wind speeds. Nevertheless, the ageostrophic wind is non-zero.

c. Implications of a purely geostrophic atmosphere

If the atmosphere was purely geostrophic, there would be no divergence or convergence since geostrophic flow is (nearly) non-divergent (see Appendix 2). Recall that divergence and convergence drive vertical motions in the atmosphere, which allow atmospheric circulation systems (cyclones and anticyclones) to grow and dissipate. Without divergence, there would be no need for meteorologists to predict the weather. Hess (1959) stated the following:

Since the wind components in geostrophic flow must be constant for an individual particle (du/dt = dv/dt = 0), and since the pressure gradient must always be in balance with the horizontal Coriolis force, it follows that the pressure gradient must be constant along the isobars (if variations of f and ρ are neglected) and constant with time. Thus, if the wind is exactly geostrophic the isobars must be straight parallel lines that are fixed in position for all time. If this were so it would be unnecessary to forecast atmospheric flow patterns.

The last sentence is especially significant, given the chosen profession of the readership of this journal. Fortunately, the synoptic-scale atmosphere is not purely geostrophic; there is constant evidence of this as atmospheric circulation systems grow and decay consistently, which implies that there is indeed divergence and convergence in the atmosphere.

3. Derivation of the Ageostrophic Wind Equations

a. Fundamental assumptions

We start with the three equations of motion for straight-line flow (no curvature):

$$\frac{du}{dt} = fv - \frac{1}{\rho}\frac{\partial p}{\partial x} + F_x \tag{5}$$

$$\frac{dv}{dt} = -fu - \frac{1}{\rho}\frac{\partial p}{\partial y} + F_y \tag{6}$$

$$\frac{dw}{dt} = -fu\cot\phi - \frac{1}{\rho}\frac{\partial p}{\partial z} - g + F_z \tag{7}$$

F_x, F_y, and F_z represent friction in the east-west, north-south, and vertical directions, respectively, and g is the acceleration due to gravity.

Since we are dealing primarily with a horizontal wind, we can neglect (roughly) the third equation. Before we do, we assume that (for synoptic-scale motions) the left-hand side (LHS) is negligible, as are the Coriolis and friction terms. This will leave us with the following:

$$0 = -\frac{1}{\rho}\frac{\partial p}{\partial z} - g \Rightarrow \frac{\partial p}{\partial z} = -\rho g \tag{8}$$

recognizable as the hydrostatic approximation, which illustrates that the vertical pressure gradient is exactly balanced by gravity. It should go without saying that this relationship works best for synoptic-scale motions (and larger).

The LHSs of (5) and (6) represent accelerations of the east-west and north-south components of the observed wind, respectively. By assuming that these accelerations are zero and that friction is negligible (which works away from the ABL), we obtain the geostrophic wind expressions shown in (2).

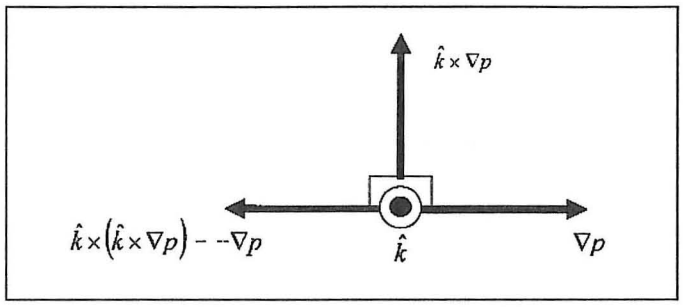

Fig. 3. Vector identity illustrating $\hat{k}$ x ($\hat{k}$ x ∇p) = ∇p. Note that $\hat{k}$ points out of the page.

But we've already stated that the atmosphere is not exactly geostrophic, but only close with respect to large-scale motions (i.e. quasi-geostrophic). This means that the LHSs of (5) and (6) are ***not*** zero, after all. Nonetheless, these accelerations are fairly small (~10^{-4} m s^{-2}) in a quasi-geostrophic atmosphere, but can no longer be ignored. These accelerations keep operational meteorologists employed.

b. Equation development

Now, start again with a (simplified) equation of motion (momentum) in vector form:

$$\frac{d\vec{V}}{dt} = \vec{P}_n + \vec{C} + \vec{F} \tag{9}$$

where the LHS represents the acceleration of the vector wind, $\vec{P}_n$ is the pressure gradient force, $\vec{C}$ represents the Coriolis force, and $\vec{F}$ is friction. More specifically, (9) can be expressed as follows:

$$\frac{d\vec{V}}{dt} = \underbrace{-\nabla\Phi}_{A} \underbrace{- f\hat{k}\times\vec{V}}_{B} \underbrace{- a\vec{V}}_{C} \tag{10}$$

where term A represents pressure gradient force, term B is Coriolis force, and term C is the frictional force. The variable 'a' in term C is a frictional coefficient, ranging from 0 (no friction) to 1 (friction completely retards motion). By assuming that the acceleration is negligible, and that the winds are above the atmospheric boundary layer, Terms A and B are left, and (10) simplifies to:

$$0 = -\nabla\Phi - f\hat{k}\times\vec{V}_g \Rightarrow f\hat{k}\times\vec{V}_g = -\nabla\Phi \tag{11}$$

Now, apply the following vector identity to (11), which is illustrated in Fig. 3:

$$\hat{k}\times\left(\hat{k}\times\vec{V}_g\right) = -\vec{V}_g \tag{12}$$

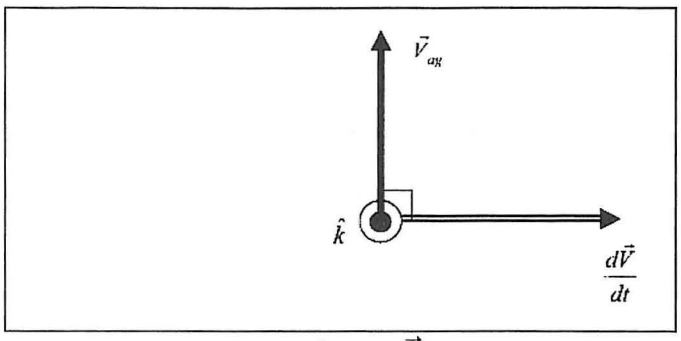

Fig. 4. Relationship between $\vec{V}_{ag}$ and $\frac{d\vec{V}}{dt}$. Note that the acceleration of the real wind is normal and to the right of the ageostrophic wind.

which yields

$$\vec{V}_g = \frac{\hat{k}}{f} \times \nabla\Phi = \frac{\hat{k}}{\rho f} \times \nabla p \tag{13}$$

Since we are dealing with the real wind (as opposed to the geostrophic wind), we bring back a form of (10), recalling that the acceleration of the real wind is not negligible (but friction is, above the ABL):

$$\frac{d\vec{V}}{dt} = -\frac{1}{\rho}\nabla p + f\vec{V} \times \hat{k} \tag{14}$$

(It should be noted that $-f\hat{k} \times \vec{V} = f\vec{V} \times \hat{k}$). Expression (13) can be rewritten as:

$$f\vec{V}_g \times \hat{k} = \frac{1}{\rho}\nabla p \tag{15}$$

and substituted into (14):

$$\frac{d\vec{V}}{dt} = -f\vec{V}_g \times \hat{k} + f\vec{V} \times \hat{k} = f\left(\vec{V} - \vec{V}_g\right) \times \hat{k} \tag{16}$$

Now recall the definition of the ageostrophic wind, way back to (1), and substitute into (16):

$$\frac{d\vec{V}}{dt} = f\vec{V}_{ag} \times \hat{k} \tag{17}$$

This expression states that the acceleration of the real wind is normal to and to the right of the ageostrophic wind (see Fig. 4). After some brief manipulation, an expression for the ageostrophic wind follows:

$$\vec{V}_{ag} = \frac{\hat{k}}{f} \times \frac{d\vec{V}}{dt} \tag{18}$$

On the RHS of (18) we have a total (Lagrangian) derivative–in this case, the total change in real wind velocity with respect to time. This derivative can be expanded into its local tendency and advective components:

$$\vec{V}_{ag} = \frac{\hat{k}}{f} \times \left[\frac{\partial\vec{V}}{\partial t} + \left(\vec{V} \cdot \nabla\right)\vec{V} + w\frac{\partial\vec{V}}{\partial z}\right] \tag{19}$$

At this point we can assume that the geostrophic momentum approximation (shown below) is valid. This is reasonable for synoptic-scale flow.

$$\left|\frac{d\vec{V}_{ag}}{dt}\right| << \left|\frac{d\vec{V}_g}{dt}\right| \tag{20}$$

This assumption transforms (19) into the following expression for the ageostrophic wind:

$$\vec{V}_{ag} = \frac{\hat{k}}{f} \times \left[\underbrace{\frac{\partial\vec{V}_g}{\partial t}}_{A} + \underbrace{\left(\vec{V} \cdot \nabla\right)\vec{V}_g}_{B} + \underbrace{w\frac{\partial\vec{V}_g}{\partial z}}_{C}\right] \tag{21}$$

Note that the second term (B) refers to the advection of the *geostrophic* wind by the *real* (geostrophic + ageostrophic) wind, since advection by the ageostrophic part of the wind may be large, especially near fronts and jets. Each term and its physical significance will be examined in the following section.

4. Examination of Individual Terms of the Ageostrophic Wind Expression

a. Term A – isallobaric wind

Term A of (21) can be expanded by substituting (3) for the geostrophic wind $\vec{V}_g$:

$$\frac{\hat{k}}{f} \times \frac{\partial\vec{V}_g}{\partial t} = \frac{\hat{k}}{f} \times \frac{\partial}{\partial t}\left(\frac{\hat{k}}{\rho f} \times \nabla p\right) \tag{22}$$

By assuming that the Coriolis parameter (f) and density (ρ) are constant, they can be pulled out from the partial derivative. The unit vector $\hat{k}$ can be moved into the derivative (it does not matter, as it is constant, too). Equation (22) then becomes the following:

$$\frac{\hat{k}}{f} \times \frac{\partial\vec{V}_g}{\partial t} = \frac{1}{\rho f^2}\frac{\partial}{\partial t}\left[\hat{k} \times \left(\hat{k} \times \nabla p\right)\right] \tag{23}$$

Recall the vector identity shown in (12), and apply it to ∇p:

$$\hat{k} \times \left(\hat{k} \times \nabla p\right) = -\nabla p \tag{24}$$

Substitution of (24) into (23) yields

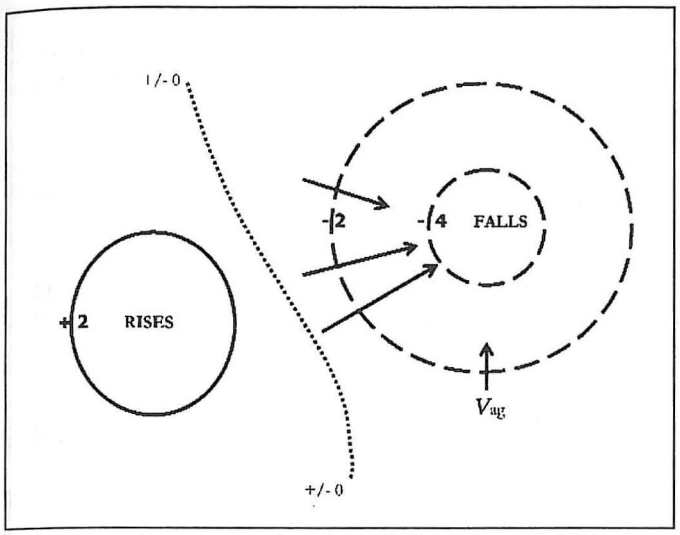

Fig. 5. Isallobaric component of the ageostrophic wind. Solid (dashed) contours represent locations of equal pressure rise (fall) over some arbitrary time period.

$$\frac{\hat{k}}{f} \times \frac{\partial \vec{V}_g}{\partial t} = \frac{1}{\rho f^2} \frac{\partial}{\partial t}\left(-\nabla p\right) \tag{25}$$

The order of differentiation is not important, so we reverse the tendency and the gradient. Expression (25) then becomes:

$$\vec{V}_{ag} = -\frac{1}{\rho f^2} \nabla\left(\frac{\partial p}{\partial t}\right) \tag{26}$$

This component of the ageostrophic wind is the *isallobaric* wind. It blows from regions of pressure rises to regions of pressure falls, from strong pressure rises to weak pressure rises, etc. (see Fig. 5). The isallobaric wind will be strong when there are strong, rapid changes in pressure (e.g., explosive cyclogenesis).

b. Term B – inertial-advective component

Now, let us focus on Term B of (21), perhaps the strangest of the three. It can be expanded into Cartesian coordinates, resulting in the following:

$$\frac{\hat{k}}{f} \times \left(\vec{V} \cdot \nabla\right)\vec{V}_g = \frac{\hat{k}}{f} \times \left[\left(\underbrace{u\frac{\partial u_g}{\partial x}}_{A} + \underbrace{v\frac{\partial u_g}{\partial y}}_{B}\right)\hat{i} + \left(\underbrace{u\frac{\partial v_g}{\partial x}}_{C} + \underbrace{v\frac{\partial v_g}{\partial y}}_{D}\right)\hat{j}\right] \tag{27}$$

This is the *inertial-advective component* of the ageostrophic wind (the horizontal advection of the *geostrophic* wind by the *real* wind). It will be strong in regions of diffluent or confluent flow, curved flow (ridges and troughs), or in the entrance/exit regions of jet streaks. Figures 6-9 show specific case examples, relating the inertial-advective component of the ageostrophic wind to the acceleration of the real wind.

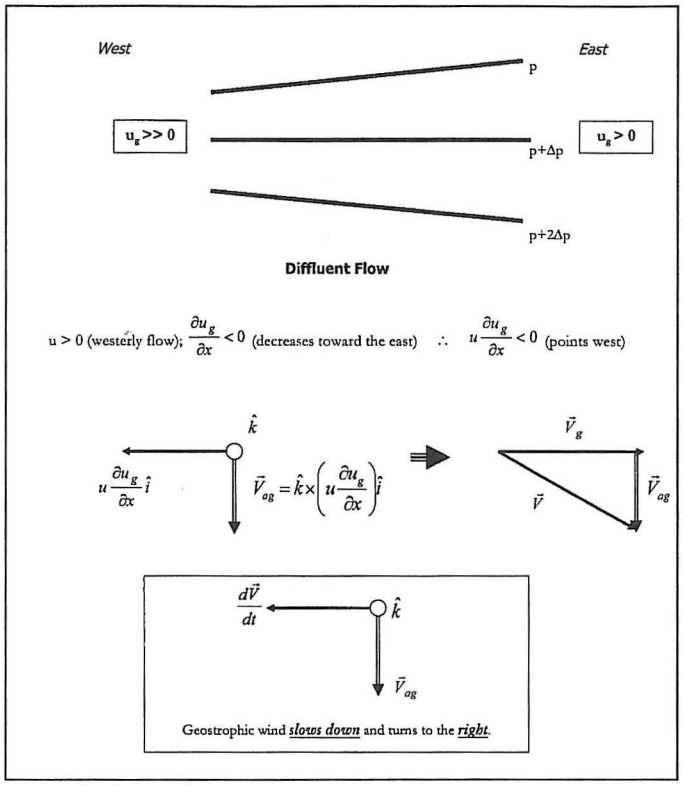

Fig. 6. Case example of the influence of the inertial-advective wind in the presence of diffluent flow. We should expect that the wind weakens as ∇p decreases downstream.

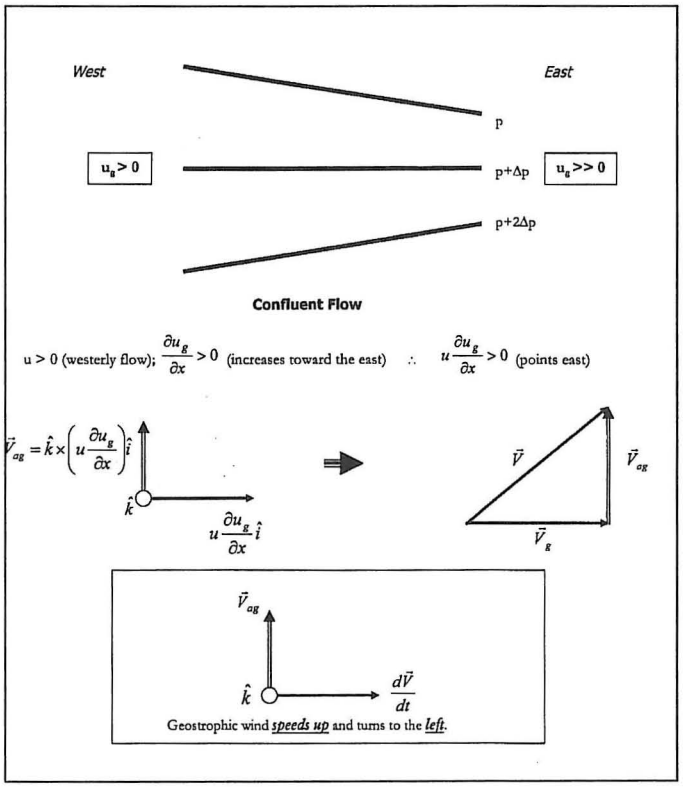

Fig. 7. Case example of the influence of the inertial-advective wind in the presence of confluent flow. We should expect that the wind strengthens as ∇p increases downstream.

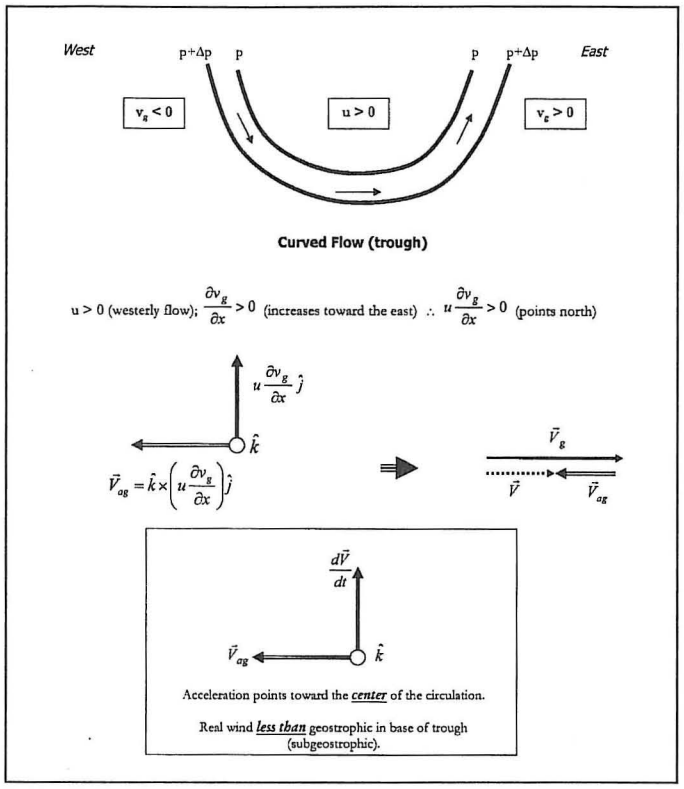

Fig. 8. Case example of the influence of the inertial-advective wind in the presence of curved flow (base of trough).

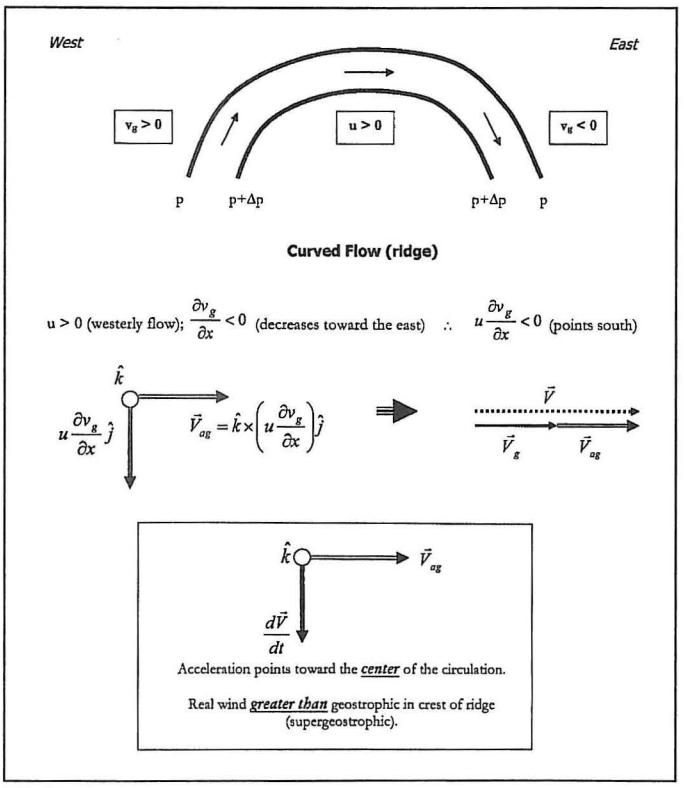

Fig. 9. Case example of the influence of the inertial-advective wind in the presence of curved flow (crest of a ridge).

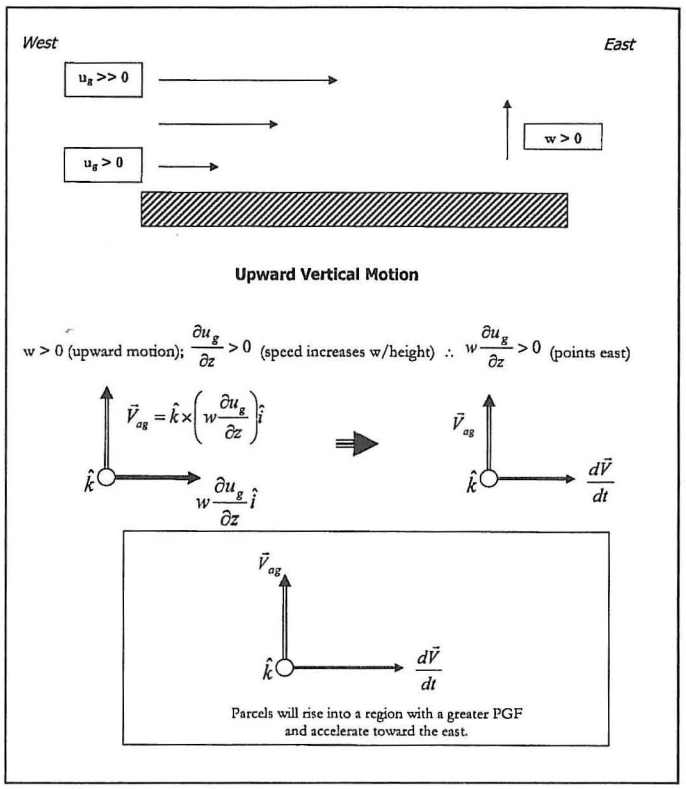

Fig. 10. Case example of the influence of the inertial-convective wind component of $\vec{V}_{ag}$.

c. Term C – inertial-convective component

Term C of (21) can be expanded in a fashion similar as Term B (see previous section):

$$\frac{\hat{k}}{f} \times w \frac{\partial \vec{V}_g}{\partial z} = \frac{\hat{k}}{f} \times w \left(\frac{\partial u_g}{\partial z} \hat{i} + \frac{\partial v_g}{\partial z} \hat{j} \right) \qquad (28)$$

(28) represents the *inertial-convective component* of the ageostrophic wind (the vertical advection of the geostrophic wind by updrafts and downdrafts). It will be strongest under conditions of strong vertical wind shear (generally found in strongly baroclinic environments) and/or strong vertical motion (upward or downward). Figure 10 illustrates this component of the ageostrophic wind.

5. 1200 UTC 1 May 2004 – An Illustration of the Ageostrophic Wind and Its Components

A brief case study is provided to illustrate the utility of the ageostrophic wind and its components. Analyses are derived from the Nested Grid Model (NGM) run initialized at 1200 UTC 30 April 2004. In particular, the 24-h output is used, as the fields depicted a well-developed cold frontal zone across the central U.S. (Fig. 11). Moreover, the 24-h solutions come from the middle of the simulation when the model is dynamically balanced. It should be noted that the case study fields are expressed on constant pressure surfaces (p-space), while the expres-

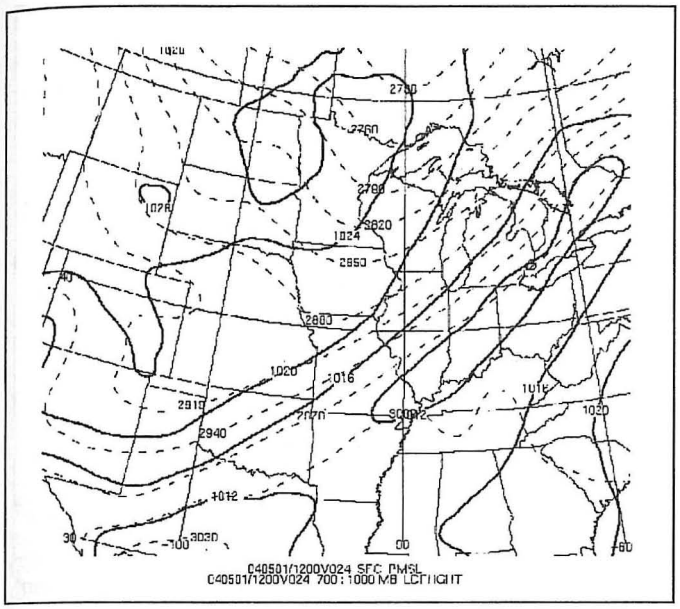

Fig. 11. NGM 24-h forecast of mean sea-level pressure (solid, hPa) and 1000-700 hPa thickness (dashed, gpm) valid at 1200 UTC 01 May 2004.

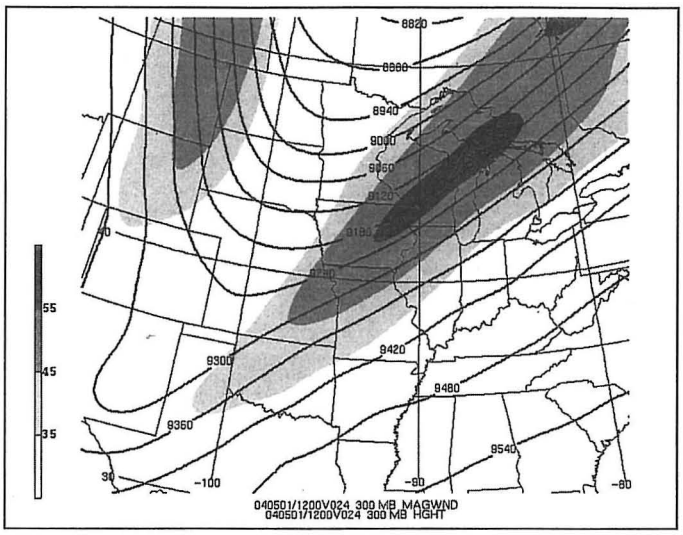

Fig. 12. NGM 24-h forecast of 300-hPa geopotential heights (solid, gpm) and isotachs (shaded ≥ 35 m s^{-1}) valid at 1200 UTC 01 May 2004.

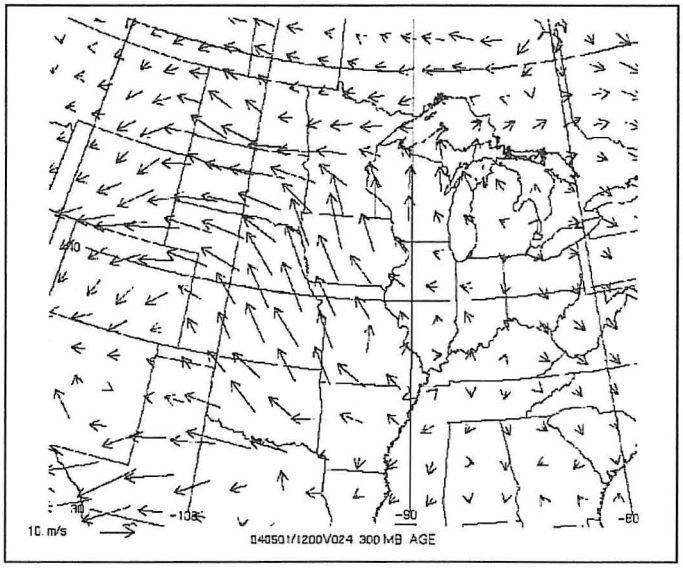

Fig. 13. NGM 24-h forecast of 300-hPa ageostrophic wind vectors valid at 1200 UTC 01 May 2004. Representative vector in lower-left corner has a magnitude of 10 m s^{-1}.

sions for the ageostrophic wind components discussed previously in the text are expressed using height as a vertical coordinate (z-space). Analogous expressions for the ageostrophic wind and its components in p-space are quite similar to those in z-space.

The NGM was chosen for this study due to its relatively coarse grid spacing (84 km @ 45°N). It was thought that with fewer grid points, the wind fields might be somewhat smoother. Nevertheless, the fields of u, v, ω, and height were subjected to a 9-point smoother before reasonable wind fields could be generated. While the inertial-advective term may be calculated with values at a single time and level, the other components of $\vec{V}_{ag}$ may not. Specifically, the isallobaric component requires a time difference in the geostrophic wind; this is accomplished using the smoothed heights at both the 18-h and 24-h forecast times. Also, the inertial-convective term requires a layer difference to account for the wind shear around the chosen layer (300 hPa); this is obtained by differencing the geostrophic wind over the 400-200 hPa layer. In general, qualitatively summing the three component vectors over the included grids leads to a reasonable approximation of the total ageostrophic wind vector, although there are locations where this relationship fails, especially in regions where the inertial-advective component is large. We acknowledge this shortcoming in the hope that the reader will accept the "spirit" of the case study's inclusion and excuse its "letter," with the understanding that the case study is included for purposes of illustration.

Examination of the 300-hPa level (Fig. 12) reveals a trough over the Great Plains with jet cores (≥ 35 m s^{-1}) over Montana and Wisconsin. The curvature present in the flow field suggests a significant inertial-advective component. The transient nature of the trough (predicted by the NGM) suggests a significant isallobaric component. Indeed, the ageostrophic winds (Fig. 13) are in excess of 10 m s^{-1} over a broad region of the central United States.

The inertial-advective component (Fig. 14) accounts for a large portion of the total $\vec{V}_{ag}$, especially over eastern Kansas and northwestern Missouri. Here, the inertial-advective is dominated by across-stream flow. A similar observation is made over eastern Wyoming, although the resultant acceleration will be opposite that over Kansas. The ageostrophic winds (Fig. 13) and their inertialadvective components over Kansas and Wyoming are good examples of the across-stream behavior in confluent and diffluent zones, respectively. The along-stream signature of enhanced cyclonic curvature is manifested best over western Texas, where the inertial-advective component points to the base of the trough.

Convergence is prevalent in the isallobaric field (Fig. 15) ahead of the trough axis, although it is most promi-

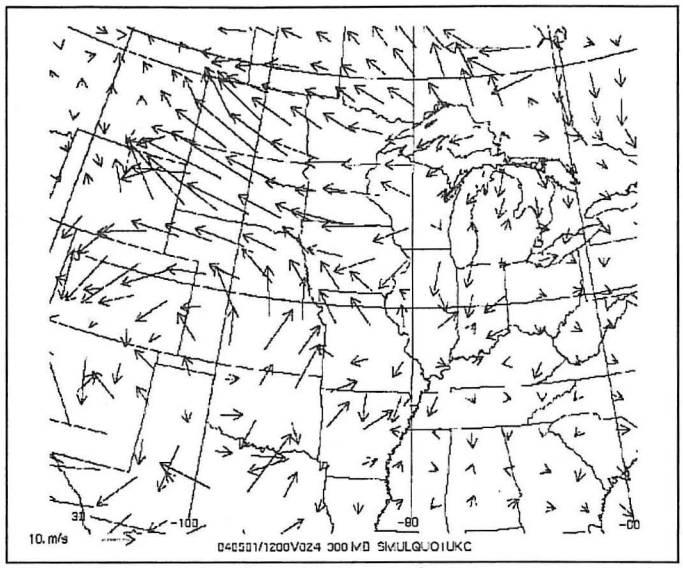

Fig. 14. As in Fig. 13, except for the inertial-advective component of the ageostrophic wind.

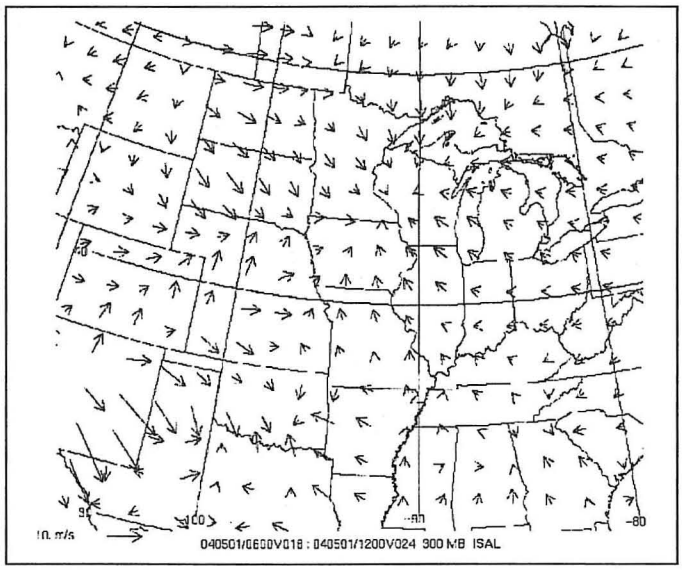

Fig. 15. As in Fig. 13, except for the isallobaric component of the ageostrophic wind.

nent over western Texas, the southern end of the trough. To the west of the 300-hPa trough axis there is a weakly divergent pattern in the vector field. This arrangement suggests rising heights to the west of the trough and falling heights ahead, exactly as predicted by the NGM.

Lastly, we examine the inertial-convective components (Fig. 16). Note the generally weak magnitude of most of the vectors, especially in comparison to the inertial-convective and isallobaric components. However, there are relatively "large" vectors over Texas near the southern end of the trough and the entrance region of the jet streak. A relatively strong change in the wind speed in the 400-200 hPa layer is acting to make the vectors as large as they are. The acceleration suggested by these vectors will be downstream, toward the northeast. This is necessary for ascending parcels in a sheared environment. As they rise, they must accelerate in order to adjust to the higher wind speeds farther aloft.

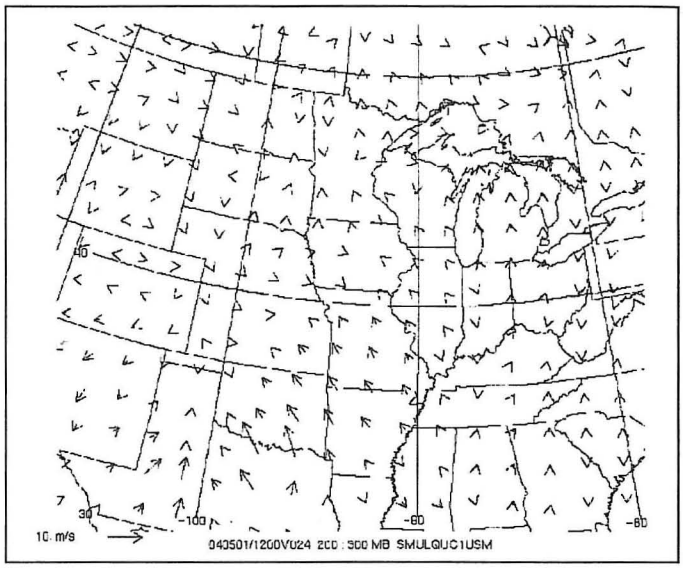

Fig. 16. As in Fig. 13, except for the inertial-convective component of the ageostrophic wind.

Of course, far more could be done with such a case study. In particular, examination of various vertical levels would be most beneficial and thorough. Our attempt here is to illustrate those concepts, which our preceding discussions sought to illuminate through theoretical treatment.

6. Discussion

This article was written to illustrate the theory and application of the ageostrophic wind. Although generally small for synoptic-scale motions, the fact that it is not exactly zero has significant implications for operational meteorology (and its practitioners), mainly the production of divergence and convergence throughout the troposphere, which control the development and diminution of midlatitude and polar weather systems.

At this point, the following question might arise: under what conditions would one expect the ageostrophic wind to be especially strong? Recall the conditions under which the geostrophic wind most closely approximates reality: straight isobars/height contours, above the ABL. As such, the ageostrophic wind is strong (and the real wind departs strongly from geostrophy) under the following conditions:

- Within the atmospheric boundary layer (where friction is strongest; e.g., Fig. 17)
- Curved flow (ridges and troughs; e.g., Fig. 18)
- Strong changes in the pressure/height fields (e.g., Fig. 19)
- Confluent or diffluent flow (e.g., Figs. 20-21)
- Entrance/exit/center regions of jet streaks (e.g., Fig. 22)

One might also wonder about the abundance of equations in this article. They can be thought of as a "shorthand" of sorts. They allow the succinct expression of physical processes and forcing mechanisms that are important in meteorology. Bluestein (1992) stated the following regarding equations, which summarizes their importance:

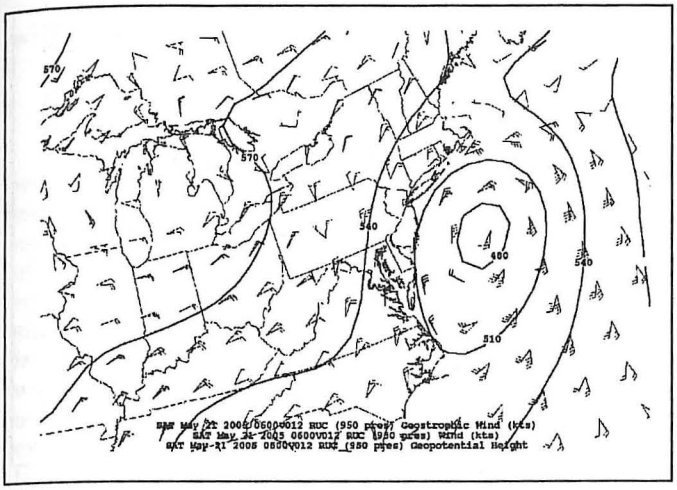

Fig. 17. An example of friction-induced departures from geostrophy. Solid contours are 950-hPa heights (gpm). 950-hPa geostrophic and actual wind barbs are in standard format, with the geostrophic wind barbs parallel to the height contours. All parameters are 12-h forecasts from the 1800 UTC 20 May 2005 run of the rapid update cycle (RUC) model, valid at 0600 UTC 21 May 2005.

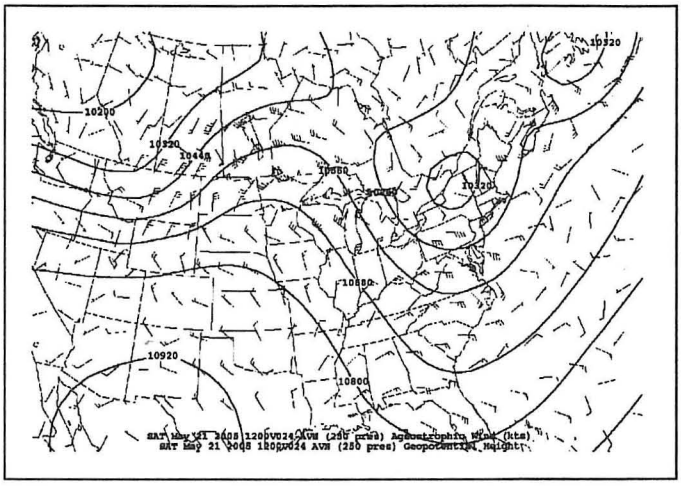

Fig. 18. An example of the ageostrophic wind in a field of curved flow. Solid contours are 250-hPa heights (gpm). 250-hPa ageostrophic wind barbs are in standard format. Note the downstream direction of the barbs (resulting in supergeostrophic flow) in the ridge across the Upper Midwest, and their upstream orientation (yielding subgeostrophic flow) in the trough over the Mid-Atlantic and Southeastern U.S. All parameters are 24-h forecasts from the 1200 UTC 20 May 2005 run of the Global Forecast System (GFS) model, valid at 1200 UTC 21 May 2005.

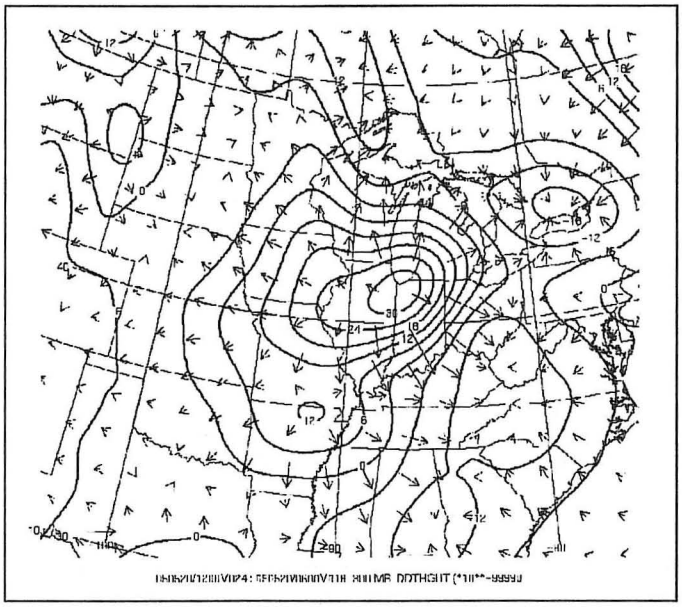

Fig. 19. An example of the isallobaric wind. Solid contours are 300-hPa height change [gpm (6 h)$^{-1}$], arrows represent 300-hPa isallobaric wind (m s^{-1}). Note the divergent vectors corresponding to -1 significant height rises near Chicago, and the converging winds associated with height falls near Lake Ontario. The isallohypses are derived from the 18- and 24-h forecasts based on the 1200 UTC 19 May 2005 run of the Eta model, valid at 1200 UTC 20 May 2005, while the isallobaric winds are derived from the 24-h forecast, valid at 1200 UTC 20 May 2005.

It is important that one not merely memorize these (or any!) equations by rote. It is much more important to understand what they mean physically. Once the physical effects of each term are understood, one can then convert the physics into mathematics and write down the equations.

Acknowledgments

The concept of this paper arose from a frequently-asked questions (FAQ) document composed by the primary author for the students of his Weather Forecasting course at SUNY Brockport. As such, he is grateful to his students, past and present. The authors wish to thank Mr. J. Kevin Lavin, NWA executive director, for his support of this article. Thanks are also due to Dr. Cecilia Miner and Ms. Cynthia Nelson, whose thorough reviews of the manuscript are responsible for numerous improvements. Lastly, the authors are deeply beholden to Dr. James T. (Doc) Moore for his expert instruction and exhaustive class materials, from which portions of this paper were derived. We dedicate this article in his memory.

Authors

Scott M. Rochette, Ph.D., is an associate professor of meteorology in the Department of the Earth Sciences at State University of New York, College at Brockport, where he also serves as Weather Center Director. He received his B.S. (1988) in meteorology from Lyndon State College, and his M.S. (1994) and Ph.D. (1998) degrees in meteorology from Saint Louis University. His teaching interests include synoptic meteorology, weather forecasting, dynamic meteorology, mesoscale meteorology, and writing in the earth sciences. His research interests include jet streak interactions, warm- and cold-season heavy precipitation, and analysis and prediction of local and regional severe weather events. Prior appointments include a visiting assistant professorship at St. Cloud State University (Minnesota) and a meteorologist/fore-

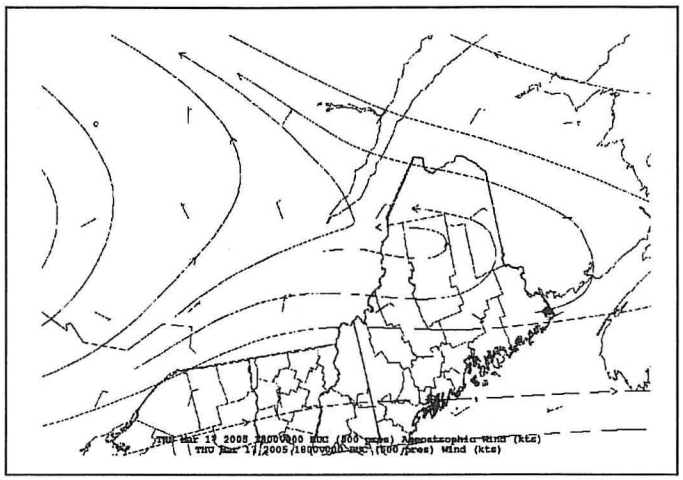

Fig. 20. An example of the ageostrophic wind in diffluent flow. Solid contours are 500-hPa streamlines. 500-hPa ageostrophic wind vectors are in standard format. Note the region of northerly ageostrophic winds in the diffluent region across eastern Quebec and northern Vermont. These fields are derived from the 00-h forecast of the 1800 UTC 17 March 2005 run of the RUC model.

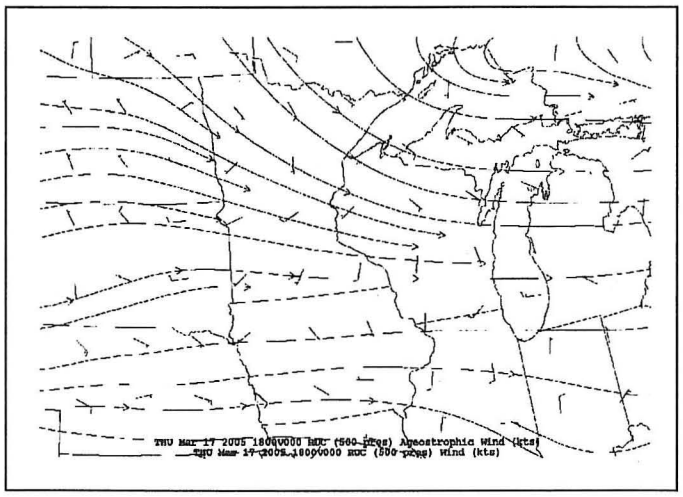

Fig. 21. As in Fig. 20, except for confluent flow. Note the southerly ageostrophic winds in the confluent region across southeastern Minnesota and western Wisconsin.

caster position at New England Weather Service (Connecticut). He served as a technical editor of *National Weather Digest* from 2003 to 2006, and continues to serve on the NWA Weather Analysis and Forecasting Committee.

Patrick S. Market, Ph.D., is an associate professor of atmospheric science in the Department of Soil, Environmental and Atmospheric Sciences at the University of Missouri-Columbia. He received a B.S. (1994) in meteorology from Millersville University of Pennsylvania, as well as M.S. (1996) and Ph.D. (1999) degrees in meteorology from Saint Louis University. His research interests include the extratropical cyclone occlusion process, jet streak/frontal morphology and propagation, heavy convective snowfall events, and precipitation efficiency. Dr. Market has held positions as a forecaster and as a certified weather observer concurrent with his

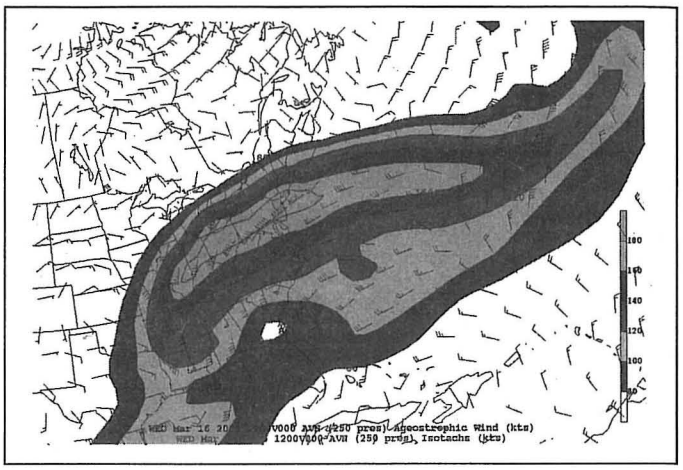

Fig. 22. An example of ageostrophic flow in the vicinity of an upper-level jet streak. Shaded bands represent 250-hPa wind speed ≥ 80 kts. 250-hPa ageostrophic winds are in standard format. Note the general southerly (northerly) cross-jet flow in the entrance (exit) region of the jet streak. These parameters are 00-h forecasts from the 1200 UTC 16 March 2005 run of the GFS model.

educational career. In the summer of 1998, he also served as a radiosonde technician during the South China Sea Monsoon Experiment. He serves as an editor of *National Weather Digest*. In addition, he serves on the NWA Weather Analysis and Forecasting Committee and oversees that body's Research Subcommittee.

References

Billingsley, D. B., 1996: What does quasi-geostrophic really mean? *Natl. Wea. Dig.*, 21:1, 21-25.

_____, 1997: Review of QG theory–Part II: The omega equation. *Natl. Wea. Dig.*, 21:2, 43-51.

_____, 1998: Review of QG theory–Part III: A different approach. *Natl. Wea. Dig.*, 22:3, 3-10.

Bluestein, H. B., 1992: *Synoptic-Dynamic Meteorology in Midlatitudes: Volume I: Principles of Kinematics and Dynamics*. Oxford University Press, 431 pp.

Hess, S. L., 1959: *Introduction to Theoretical Meteorology*. Holt, Rinehart and Winston, 362 pp.

Wallace, J. M., and P. V. Hobbs, 1977: *Atmospheric Science: An Introductory Survey*. Academic Press, 467 pp.

Appendix 1: Review of Vector Functions

The use of vector notation and functions throughout this article is meant to simplify the underlying mathematics. We provide a brief refresher of vectors and vector functions. A *vector* is defined as a quantity that has both magnitude and direction (*cf.* scalar, which has magnitude only). Perhaps the easiest (and most appropriate to this paper) vector quantity to visualize is wind velocity $\vec{V}$,

which has direction and speed (magnitude):

$$\vec{V} = u\hat{i} + v\hat{j} + w\hat{k} \tag{A1}$$

where u, v, and w represent the wind speeds in the east-west, north-south, and vertical directions, respectively, and $\hat{i}, \hat{j}$, and $\hat{k}$ and represent the unit vectors (magnitude of 1) in the east-west, northsouth, and vertical directions, respectively. This particular example is a three-dimensional wind, which is quite often partitioned into its horizontal and vertical components. A horizontal wind vector would be comprised of the first two right-hand-side terms of (A1). The geostrophic or ageostrophic winds would be expressed by the addition of a subscript '*g*' or '*a*,' respectively, to each component.

The *gradient* ('del') operator is commonly used in meteorology and it represents spatial changes in a given atmospheric property. If we assume an arbitrary meteorological scalar property A, the three-dimensional gradient of A would be given as the following:

$$\nabla A = \frac{\partial A}{\partial x}\hat{i} + \frac{\partial A}{\partial y}\hat{j} + \frac{\partial A}{\partial z}\hat{k} \tag{A2}$$

Note that the gradient of a function is a vector quantity.

The two most common multiplication operations involving vector quantities are the dot product and cross product. The dot product of two vectors is a scalar quantity; if we assume two arbitrary vectors $\vec{A}$ and $\vec{B}$, the dot product is expressed as such:

$$\vec{A} \cdot \vec{B} = \left|\vec{A}\right|\left|\vec{B}\right|\cos\alpha \tag{A3}$$

In other words, the dot product of vectors $\vec{A}$ and $\vec{B}$ is the product of the two vectors' magnitudes, multiplied by the cosine of the angle between the two vectors (a). Meteorological applications of the dot product include divergence of the wind field:

$$\nabla \cdot \vec{V} = \frac{\partial u}{\partial x} + \frac{\partial v}{\partial y} + \frac{\partial w}{\partial z} \tag{A4}$$

and temperature advection by the wind:

$$-\vec{V} \cdot \nabla T = -u\frac{\partial T}{\partial x} - v\frac{\partial T}{\partial y} - w\frac{\partial T}{\partial z} \tag{A5}$$

The cross product of two vectors is somewhat more involved. It is also a vector quantity. Assuming the two arbitrary vectors described previously, the magnitude of their cross product can be expressed as the following:

$$\left|\vec{A} \times \vec{B}\right| = \left|\vec{A}\right|\left|\vec{B}\right|\sin\alpha \tag{A6}$$

which is similar to the formulation of the dot product. The cross product of the two vectors (assuming each vector has three dimensions) can be expressed as the determinant of the following matrix:

$$\vec{A} \times \vec{B} = \begin{vmatrix} \hat{i} & \hat{j} & \hat{k} \\ A_x & A_y & A_z \\ B_x & B_y & B_z \end{vmatrix} \tag{A7}$$
$$= \left(A_yB_z - A_zB_y\right)\hat{i} - \left(A_xB_z - A_zB_x\right)\hat{j} + \left(A_xB_y - A_yB_x\right)\hat{k}$$

The cross product of two vectors is normal to the plane of the two vectors. Meteorological applications of the cross product include three-dimensional relative vorticity (given as the curl of the wind velocity field $\nabla \times \vec{V}$); in this example, we illustrate the vorticity about a vertical axis only:

$$\zeta = \hat{k} \cdot \left(\nabla \times \vec{V}\right) = \frac{\partial v}{\partial x} - \frac{\partial u}{\partial y} \tag{A8}$$

Note that the 3D vorticity itself is a vector quantity, but taking its dot product with the vertical unit vector yields the (familiar) expression for relative vorticity.

Appendix 2: Proof of the Non-Divergent Nature of the Geostrophic Wind

Start with the expressions of u_g and v_g, based loosely on (2), except we will use geopotential ($\Phi = gz$) in lieu of pressure; this allows the elimination of density (ρ):

$$u_g = -\frac{1}{f}\frac{\partial \Phi}{\partial y}$$
$$v_g = \frac{1}{f}\frac{\partial \Phi}{\partial x} \tag{A9}$$

Now, recall the definition of divergence:

$$Div = \nabla \cdot \vec{V} = \frac{\partial u}{\partial x} + \frac{\partial v}{\partial y} \tag{A10}$$

Plug (A9) into (A10):

$$\nabla \cdot \vec{V}_g = \frac{\partial u_g}{\partial x} + \frac{\partial v_g}{\partial y} \tag{A11}$$

and then (A9) into (A11):

$$\nabla \cdot \vec{V}_g = \frac{\partial}{\partial x}\left(-\frac{1}{f}\frac{\partial \Phi}{\partial y}\right) + \frac{\partial}{\partial y}\left(\frac{1}{f}\frac{\partial \Phi}{\partial x}\right) \tag{A12}$$

which becomes:

$$\nabla \cdot \vec{V}_g = -\frac{1}{f}\frac{\partial}{\partial x}\left(\frac{\partial \Phi}{\partial y}\right) - \frac{\partial \Phi}{\partial y}\frac{\partial}{\partial x}\left(\frac{1}{f}\right) + \frac{1}{f}\frac{\partial}{\partial y}\left(\frac{\partial \Phi}{\partial x}\right) + \frac{\partial \Phi}{\partial x}\frac{\partial}{\partial y}\left(\frac{1}{f}\right) \quad \text{(A13)}$$

or:

$$\nabla \cdot \vec{V}_g = -\frac{1}{f}\frac{\partial^2 \Phi}{\partial x \partial y} - \frac{\partial \Phi}{\partial y}\frac{\partial}{\partial x}\left(\frac{1}{f}\right) + \frac{1}{f}\frac{\partial^2 \Phi}{\partial x \partial y} + \frac{\partial \Phi}{\partial x}\frac{\partial}{\partial y}\left(\frac{1}{f}\right) \quad \text{(A14)}$$

Note that the first and third terms of the RHS of (A14) sum to zero, and that f is constant in the eastwest (x) direction, so the second term goes to zero, which leaves the following:

$$\nabla \cdot \vec{V}_g = \frac{\partial \Phi}{\partial x}\frac{\partial}{\partial y}\left(\frac{1}{f}\right) \quad \text{(A15)}$$

Now, perform the differentiation on the RHS of (A15):

$$\nabla \cdot \vec{V}_g = -\frac{1}{f^2}\frac{\partial f}{\partial y}\frac{\partial \Phi}{\partial x} \quad \text{(A16)}$$

We can define $\beta = \frac{\partial f}{\partial y}$, which describes the change in the Coriolis parameter in the north-south direction (from equator to pole). Also, recall (A9) and substitute into (A16):

$$\nabla \cdot \vec{V}_g = -\frac{\beta}{f} v_g \quad \text{(A17)}$$

Through scale analysis, the divergence of the geostrophic wind can be evaluated by assigning typical values to the quantities on the RHS of (A17):

$$\beta \sim 10^{-11}\ (\text{m s})^{-1} \qquad f \sim 10^{-4}\ \text{s}^{-1} \qquad v_g \sim 10\ \text{m s}^{-1}$$

$$\nabla \cdot \vec{V}_g \sim \frac{\left[10^{-11}\ (ms)^{-1}\right]\left[10\ ms^{-1}\right]}{\left[10^{-4}\ s^{-1}\right]} \sim 10^{-6}\ s^{-1} \quad \text{(A18)}$$

Typical values of divergence for synoptic-scale flows are ~ 10^{-5} s^{-1}, an order of magnitude larger than that of the geostrophic wind. As such, the divergence of the geostrophic wind is assumed to be negligible.